J|A|C|S
ARTICLES
Published on Web 12/09/2004

Thermodynamic Guidelines for the Design of Bimetallic Catalysts for Oxygen Electroreduction and Rapid Screening by Scanning Electrochemical Microscopy. M−Co (M: Pd, Ag, Au)

José L. Fernández, Darren A. Walsh, and Allen J. Bard*

Contribution from the Department of Chemistry and Biochemistry, University of Texas at Austin, Austin, Texas 78712

Received August 19, 2004; E-mail: ajbard@mail.utexas.edu

Abstract: We propose guidelines for the design of improved bimetallic (and related) electrocatalysts for the oxygen reduction reaction (ORR) in acidic media. This guide is based on simple thermodynamic principles assuming a simple mechanism where one metal breaks the oxygen−oxygen bond of molecular O_2 and the other metal acts to reduce the resulting adsorbed atomic oxygen. Analysis of the Gibbs free energies of these two reactions guides the selection of combinations of metals that can produce alloy surfaces with enhanced activity for the ORR when compared to the constituent metals. Selected systems have been tested by fabricating arrays of metallic catalysts consisting of various binary and ternary combinations of Pd, Au, Ag, and Co deposited on glassy carbon (GC) substrates. The electrocatalytic activity of these materials for the ORR in acidic medium was examined using scanning electrochemical microscopy (SECM) in a new rapid-imaging mode. This was used to rapidly screen arrays covering a wide range of catalyst compositions for their activity for the ORR in 0.5 M H_2SO_4. Using the SECM technique, we have identified combinations of metals with enhanced electrocatalytic activities when compared with the constituent, pure metals. Addition of Co to Pd, Au, and Ag clearly decreases the ORR overpotential, in agreement with the proposed model. Catalyst spots that exhibited enhanced electrocatalytic activity in the SECM screening technique were then examined using classical rotating disk electrode (RDE) experiments. The activity of carbon black supported catalyst mixtures on a GC RDE and the electrocatalytic activity determined using the SECM screening technique showed excellent agreement. C/Pd−Co electrodes (10−30% Co) exhibited remarkable activity for ORR catalysis, close to that of carbon-supported Pt.

Introduction

The search for abundant, inexpensive, and efficient electrocatalytic materials as substitutes for Pt-based oxygen cathodes in polymer electrolyte membrane fuel cells (PEMFC) is currently an active area of research. Efforts are also under way to increase the heterogeneous electron-transfer kinetics and the utilization of Pt, for example, by modification of carbon supports[1] and novel platinum deposition techniques[2] to increase the effective catalytic area (thereby decreasing the loading of precious metal). Novel approaches toward improving ORR electrocatalysis have also included replacement of some platinum with an alternative, less expensive metal (e.g., Co, Cr, Ni).[3] While this approach has yielded some materials that have improved electrocatalytic activities and are less expensive than pure Pt catalysts, the costs associated with these materials are still rather prohibitive for full exploitation of fuel cell technology. Probably the most ambitious approach to this problem and with the greatest potential is to completely remove Pt from these systems and replace it with less expensive materials, while retaining catalytic activity at least equal to that of Pt. Some advances using this approach have been made in recent years. For example, electroreduction of oxygen at non-platinum metallic combinations,[4] inorganic and organometallic complexes,[5] transition metal oxides,[6] calchogenides,[7] and enzyme electrodes[8] have been studied.

Despite the extensive research that has been carried out in this area, the detailed mechanism of the ORR, even at Pt, is

(1) (a) Hou, Z.; Yi, B.; Zhang, H. *Electrochem. Solid State Lett.* **2003**, *6*, A232. (b) Wang, C.; Mahesh, W.; Wang, X.; Tang, J. M.; Haddon, R. C.; Yan, Y. *Nano Lett.* **2004**, *4*, 345.

(2) (a) Zhang, J.; Mo, Y.; Vukmirovic, M. B.; Klie, R.; Sasaki, K.; Adzic, R. R. *J. Phys. Chem. B* **2004**, *108*, 10955. (b) Van Brussel, M.; Kokkinidis, G.; Hubin, A.; Buess-Herman, C. *Electrochim. Acta* **2003**, *48*, 3909.

(3) (a) Paulus, U. A.; Wokaun, A.; Scherer, G. G.; Schmidt, T. J.; Stamenkovic, V.; Radmilovic, V.; Markovic, N. M.; Ross, P. N. *J. Phys. Chem. B* **2002**, *106*, 4181. (b) Yang, H.; Alonso-Vante, N.; Léger, J.-M.; Lamy, C. *J. Phys. Chem. B* **2004**, *108*, 1938. (c) Mukerjee, S.; Srinivasan, S. *J. Electroanal. Chem.* **1993**, *357*, 201. (d) Xiong, L.; Kankan, A. M.; Manthiram, A. *Electrochem. Commun.* **2002**, *4*, 898.

(4) (a) Rivera-Noriega, R.; Castillo-Hernández, N.; Soto-Guzman, A. B.; Solorza-Feria, O. *Int. J. Hydrogen Energy* **2002**, *27*, 457. (b) Ye, S.; Vijh, A. K. *Electrochem. Commun.* **2003**, *5*, 272.

(5) (a) Zagal, J.; Páez, M.; Tanaka, A. A.; dos Santos, J. R.; Linkous, C. A. *J. Electroanal. Chem.* **1992**, *339*, 13. (b) Schulenburg, H.; Stankov, S.; Schünemann, V.; Radnik, J.; Dorbandt, I.; Fiechter, S.; Bogdanoff, P.; Tributsch, H. *J. Phys. Chem. B* **2003**, *107*, 9034. (c) Sawai, K.; Suzuki, N. *J. Electrochem. Soc.* **2004**, *151*, A682 (d) Collman, J. P.; Denisevich, P.; Konai, Y.; Marrocco, M.; Koval, C.; Anson, F. C. *J. Am. Chem. Soc.* **1980**, *102*, 6027.

(6) (a) Zen, J.-M.; Manoharan, R.; Goodenough, J. B. *J. Appl. Electrochem.* **1992**, *22*, 140. (b) Zen, J.-M.; Wang, C.-B. *J. Electrochem. Soc.* **1994**, *141*, L51.

(7) González-Cruz, R.; Solorza-Feria, O. *J. Solid State Electrochem.* **2003**, *7*, 289.

10.1021/ja0449729 CCC: $30.25

still uncertain.[9] The number of possible elementary steps and mechanistic routes in the reduction of O_2 to H_2O is vast, since it involves four electron transfers, four proton transfers, and O−O bond cleavage. Adsorption of O_2 and a wide spectrum of oxygenated adsorbed intermediates probably also occurs, further complicating kinetic treatments of experimental data. Quantum mechanical calculations (e.g., ASED-MO, DFT)[10−12] are being applied to determinate optimal structures and adsorption energies and to predict synergetic effects in multicomponent model systems. However, the complexity of the mechanism makes it difficult to identify possible routes to improved electrocatalysts via purely mechanistic analysis. This complexity has led to the application of high throughput, combinatorial screening methods in the search for novel metallic electrocatalysts.[13] For example, Mallouk and co-workers have shown that a large number of catalysts can be screened simultaneously using an optical fluorescence technique detecting proton production on deposited arrays of catalyst inks spanning a range of compositions onto carbon substrates.[14] However, this approach cannot provide any insight into the quantitative electrochemical behavior. Upon detection of a possible candidate catalyst using the optical method, the material must be prepared in bulk and applied to an electrode surface and the electrochemical behavior examined.[15] Individually addressable array electrodes are also being investigated as rapid screening devices for novel electrocatalytic materials.[16−18] For example, methanol oxidation was studied using an individually addressable 25-electrode fuel cell device. Recently, SECM and combinations of SECM with other analytical methods have been proposed by Hillier and co-workers as reliable techniques for fuel cell anode screening, employing either hydrogen or methanol oxidation.[19] Moreover, we described an SECM method for studying ORR electrocatalysts.[20] Using the tip generation-substrate collection (TG-SC) mode, we could probe the ORR electrocatalytic activity of a number of catalyst spots, including highly dispersed Pt and Ru. Importantly, this approach can yield a rapid screening method for testing large arrays of multicomponent, metallic electrocatalyst spots of varying compositions.

This contribution contains four parts. (1) We propose simple selection guidelines for the selection of possible metallic catalyst candidates for the ORR. (2) We describe a method to generate large candidate arrays of different compositions. (3) Using our guidelines, we have selected various combinations of metals and demonstrate the use of SECM as a rapid activity screening technique to obtain quantitative electrochemical information about the catalyst mixtures. (4) We use the most promising compositions with a carbon support on a RDE and show that the results are in good agreement with the array results. Arrays of multimetallic catalyst spots with varying concentrations of metals on each spot have been prepared on carbon by chemical reduction of salt precursors deposited automatically under computer control. The use of SECM to measure the electrocatalytic activity of each catalyst spot is then described, and the effects of varying metal concentrations within each catalyst spot are illustrated. Using this approach, we have identified catalysts with relatively high activity for the ORR in acidic media. Current−potential curves of carbon-supported catalysts using the RDE configuration allowed a direct comparison of the proposed catalysts with Pt.

Experimental Section

Chemicals. GC plates (1 mm thick, 50 × 50 mm^2) were purchased from Alfa Aesar (Ward Hill, MA). Prior to use, the GC plates were cut into small squares to produce the GC substrates (1 mm thick, 15 × 15 mm^2). $(NH_4)_2PdCl_4$ (Aldrich, Milwaukee, WI), $HAuCl_4$ (Alfa Aesar, Ward Hill, MA), $AgNO_3$ (Strem Chemicals, Newburyport, MA), $Co(NO_3)_2(H_2O)_6$ (Aldrich, Milwaukee, WI), $Cu(NO_3)_2$ (Spectrum Chemical, Gardena, CA), glycerol (Alfa Aesar, Ward Hill, MA), and sulfuric acid (98%, Alfa Aesar, Ward Hill, MA) were all of reagent grade and were used as received. Reagent solutions were prepared using Milli-Q water (Millipore Co., Bedford, MA).

Preparation of Catalyst Spots. Catalyst spots consisting of mixtures of Pd, Ag, Au, and Co (or Cu) arranged in high-density arrays were prepared on GC by reduction of metal salt precursors with hydrogen. Solutions containing 0.3 M metal were prepared by dissolving the metal salt in water−glycerol (3:1). Binary and ternary arrays of spots containing mixtures of these solutions were deposited on GC plates using a piezo-based microarray dispenser. A commercial piezo-dispenser MicroJet AB-01−60 (MicroFab, Plano, TX), capable of dispensing picoliter-sized droplets by application of potential pulses, was installed onto a plotter head (Houston Instruments DMP-5, Houston, TX) to control its position with a resolution of 100 μm/step (Figure 1a). Typically, pulses of 50−60 V and 25 μs were applied to the piezo-dispenser using a DAQ board (Keithley Series 500, Cleveland, OH) coupled to a high voltage DC Op Amp (Burleigh PZ-70, Fisher, NY) to eject reproducible single drops of ∼100 pL. The mixtures were prepared in situ on each spot. Different quantities of each component precursor were dispensed individually at each spot (Figure 1b). Initially, the dispenser was filled with the solution of component 1. Different numbers of drops at each location were then dispensed, depending on the desired composition of each spot. The dispenser was then emptied, washed out thoroughly, and refilled with a solution of component 2. Specific numbers of drops of component 2 were then dispensed onto the pre-existing spots containing component 1. The cycle was then repeated as many times as necessary to achieve the desired compositions of the catalyst spots. The total number of moles of metal on each catalyst spot was maintained constant. Finally, the array of catalyst mixtures was agitated for 5 min using a Vortex Genie 2 agitator (Fisher, Pittsburgh, PA) to facilitate thorough mixing of the components on each spot. The array was dried at 150 °C under argon for 30 min and immediately reduced under hydrogen (1 atm) at 350 °C for 1 h using a tube furnace (Barnstead International, Dubuque, IA). In the case of the binary arrays, each composition was prepared 3 times to check the reproducibility of the catalyst spot preparation.

Rotating Disk Electrode (RDE) Preparation. Supported catalysts were prepared on carbon black with a metal loading of 20 wt %.

(8) (a) Calabrese Barton, S.; Kim, H.-H.; Binyamin, G.; Zhang, Y.; Heller, A. *J. Phys. Chem. B* **2001**, *105*, 11917. (b) Mano, N.; Kim, H.-H.; Zhang, Y.; Heller, A. *J. Am. Chem. Soc.* **2002**, *124*, 6480. (c) Mano, N.; Fernández, J. L.; Kim, Y.; Shin, W.; Bard, A. J.; Heller, A. *J. Am. Chem. Soc.* **2003**, *125*, 15290.
(9) Adžić, R. In *Electrocatalysis*; Lipkowski, J., Ross, P. N., Eds.; Wiley-VCH: New York, 1998; Chapter 5, p 197.
(10) Anderson, A. B. *Electrochim. Acta* **2002**, *47*, 3759.
(11) Balbuena, P. B.; Altomare, D.; Vadlamani, N.; Bingi, S.; Agapito, L. A.; Seminario, J. M. *J. Phys. Chem. A* **2004**, *108*, 6378.
(12) Xu, Y.; Ruban, A. V.; Mavrikakis, M. *J. Am. Chem. Soc.* **2004**, *126*, 4717.
(13) Mallouk, T. E.; Smotkin, E. S. In *Handbook of Fuel Cells − Fundamental and Applications*; Vielstich, W., Lamm, A., Gasteiger, H. A., Eds.; John Wiley & Sons: Hoboken, New Jersey, 2003; Vol. 2, Part 3, p 334.
(14) Reddington, E.; Sapienza, A.; Gurau, B.; Viswanathan, R.; Sarangapani, S.; Smotkin, E. S.; Mallouk, T. E. *Science* **1998**, *280*, 1735.
(15) Gurau, B.; Viswanathan, R.; Lafrenz, T. J.; Liu, R.; Ley, K. L.; Smotkin, E. S.; Reddington, E.; Sapienza, A.; Chan, B. C.; Mallouk, T. E.; Sarangapani, S. *J. Phys. Chem. B* **1998**, *102*, 9997.
(16) Liu, R.; Smotkin, E. S. *J. Electroanal. Chem.* **2002**, *535*, 49.
(17) Strasser, P.; Fan, Q.; Devenney, M.; Weinberg, W. H.; Liu, P.; Nørskov, J. K. *J. Phys. Chem. B* **2003**, *107*, 11013.
(18) Guerin, S.; Hayden, B. E.; Lee, C. E.; Mormiche, C.; Owen, J. R.; Russell, A. E. *J. Comb. Chem.* **2004**, *6*, 149.
(19) (a) Jayaraman, S.; Hillier, A. C. *J. Comb. Chem.* **2004**, *6*, 27. (b) Jambunathan, K.; Jayaraman, S.; Hillier, A. C. *Langmuir* **2004**, *20*, 1856. (c) Jayaraman, S.; Hillier, A. C. *J. Phys. Chem. B* **2003**, *107*, 5221. (d) Jambunathan, K.; Hillier, A. C. *J. Electrochem. Soc.* **2003**, *150*, E312.
(20) Fernández, J. L.; Bard, A. J. *Anal. Chem.* **2003**, *75*, 2967.

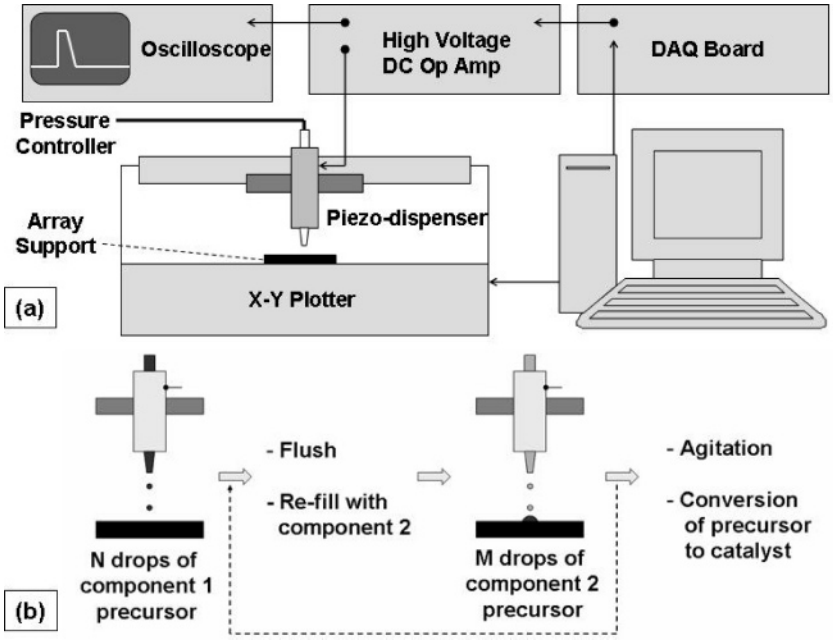

Figure 1. (a) Schematic of the setup for preparation of catalyst spots. (b) Sequence of steps for the deposition of catalyst precursor solutions for in situ preparation of multicomponent spots.

Typically, about 16 mg of Vulcan XC72R (Cabot Co., Billerica, MA) was dispersed in 5 mL of the metal salts in a water−ethanol (1:4) solution. This suspension was then agitated ultrasonically for 30 min and dried in air at 87 °C. The dried solid was placed in a porcelain boat and heated under hydrogen (1 atm) at 350 °C for 1 h in a tube furnace (Barnstead International, Dubuque, IA). The solid was then washed thoroughly with water, filtered, and dried in air. An ink of this powder was made by dispersing 8 mg in 200 μL of a 5 wt % Nafion alcoholic solution (Aldrich, Milwaukee, WI) and agitated ultrasonically for 15 min. Then 0.3 μL of this ink was deposited on a 3 mm diameter (0.071 cm^2) GC RDE (Pine Instruments, Grove City, PA) and dried for 30 s at 40 °C. The metal loading was 34 $\mu g\ cm^{-2}$.

RDE experiments were performed using a standard three-electrode cell configuration employing a platinum wire counter electrode and a Hg/Hg_2SO_4 reference electrode. A CH model 660 potentiostat (CH Instruments, Austin, TX) was employed for electrochemical measurements. In all experiments, the RDE was rotated at 2000 rpm using a Pine Instruments Analytical Rotator Model ASR2 (Pine Instruments, Grove City, PA). Rotating disk polarization curves were recorded in O_2-saturated 0.5 M H_2SO_4 with a constant flow of O_2 (1 atm) through the electrolyte at a potential sweep rate of 10 mV s^{-1}.

Scanning Electrochemical Microscopy. To avoid possible contamination of the catalyst spots with Pt from anodic dissolution of Pt SECM tips, tungsten or Au tips were used to generate oxygen during the ORR TG-SC measurements. The SECM probe tips were constructed by heat-sealing Au or tungsten wires in borosilicate glass capillaries under vacuum, followed by polishing and sharpening as previously described.[21] Briefly, a 25 μm diameter W (Alfa) or Au (Aldrich) wire was heat-sealed in a borosilicate glass capillary (O.D./I.D. = 2.0/0.9 mm) under vacuum. The bottom cross section was polished with sandpaper until the metal disk was exposed. The tip was then polished with a sequence of alumina (from 1.0 to 0.05 μm) and sharpened until an RG of about 5 was obtained. SECM measurements were performed using a PC-controlled CHI model 900 SECM (CH Instruments, Austin, TX) employing piezo inchworms (Burleigh Instruments Inc., Fishers, NY) to control the $x-y-z$ displacement. Constant tip-current TG-SC measurements were performed by controlling the substrate potential using the SECM and controlling the tip current using a 9 V battery power source between the tip (positive) and the auxiliary electrode, as described previously.[20] A Hg/Hg_2SO_4 reference electrode and a Au wire (diameter 0.5 mm) were used as reference and auxiliary electrodes, respectively. The SECM cell was carefully designed to reduce the sample tilt. The GC plate supporting the array was laid on top of a copper stripe (1 × 5 cm^2) placed on a flat acrylic base. The Teflon cell with a 1 cm diameter aperture containing an FETFE O-ring was then placed on top of the GC plate and tightened using two connecting screws. Thus, the array was exposed to the electrolyte, 0.5 M H_2SO_4. This cell was mounted on top of the regular SECM instrument stage. It was verified by SECM feedback scans that the tilt of this setup was $\Delta z/\Delta x$(or y) < 1.5 μm/mm. Note that images obtained in TG-SC mode are much less sensitive to variations in the tip−substrate distance than, for example, those obtained using feedback mode SECM.[20] The SECM tip was translated toward the substrate surface using conventional feedback mode SECM,[21] employing the oxygen reduction reaction at the SECM tip to monitor the approach of the tip to the GC surface through negative feedback. Using the feedback approach curve, the tip−substrate distance was set at 30 μm and the electrolyte solution was then deoxygenated using argon for 30 min before performing SECM imaging. A blanket of argon was maintained over the electrolyte solution at all times during the experiment to avoid interference from atmospheric oxygen. The SECM tip, held 30 μm from the GC surface, was scanned in the $x-y$ plane (x long direction) while electrogenerating O_2 from H_2O at constant current. By scanning at step intervals of 50 μm every 0.2 s, areas of 7 × 7 mm^2 could be screened in about 5 h. The substrate array potential (E_S) was held at different values where activity for O_2 reduction was detected on some spots. The substrate current (i_S), measured as a function of tip position to produce the SECM image, was larger when the O_2-generating tip passed over the more active spots. Therefore, the magnitude of the substrate current was used as a direct measure of the electrocatalytic activity of each catalyst spot. By plotting the steady state i_S values as functions of potential, polarization curves for each spot could be obtained.

Thermodynamic Principles

The detailed mechanism for oxygen reduction in acidic media remains poorly understood, although the first step probably involves the adsorption of molecular oxygen on the metal surface sites[9] or electron transfer to the O_2 molecule. In

(21) Bard, A. J. In *Scanning Electrochemical Microscopy*; Bard, A. J., Mirkin, M. V., Eds.; Marcel Dekker: New York, 2001.

the so-called "peroxide pathway," as found with Hg, Au, and C, the first electroreduction step leads to the formation of superoxide ion ($O_2^{\bullet-}$).[22]

$$O_2 + e \rightleftarrows O_2^{\bullet-} \quad (1)$$

The $E°$ for this reaction is −0.284 V vs NHE, well negative of the $E°$ of the 4e reduction to water, 1.23 V vs NHE. While the potential where this reaction occurs will be shifted to more positive values by a fast following reaction of $O_2^{\bullet-}$, one is limited in the extent of this shift by the decrease in the heterogeneous electron-transfer rate for eq 1.[23] Thus, if this pathway is to be important in electrocatalysis at the needed positive potentials, strong adsorption of the $O_2^{\bullet-}$ must be important. Moreover, to attain the 4e pathway to water, any hydrogen peroxide that is formed by the superoxide intermediate route[24] would have to undergo rapid 2e reduction to water or decomposition to water and O_2 as the step that accomplishes O−O bond cleavage.

The alternative path (the so-called "direct route") to the 4e reduction involves an initial dissociative chemisorption,[25] eq 2, involving the splitting of the O−O bond to form adsorbed oxygen atoms ($O^{\bullet}$).

$$2M + O_2 \rightleftarrows 2MO \quad (2)$$

The adsorbed oxygen atoms are then electroreduced to water according to eq 3, which actually involves a series of several elementary steps.

$$2MO + 4H^+ + 4e \rightleftarrows 2M + 2H_2O \quad (3)$$

In a sense, this can be thought of as the direct "oxidation" of metal, M, followed by the electrochemical reduction of the oxide. From a simple analysis of these two reactions, we can infer that metals that favor bond cleavage will stabilize the intermediate (MO), resulting in a highly negative reduction potential that is generally too negative to be of interest in power source applications. Figure 2 shows tabulated data[26,27] for the Gibbs free energy for reaction 2 (assuming bulk oxide) versus the standard potential for reaction 3 for a number of metals and oxides of metals in the +2 oxidation state, but it could be similarly extended to include other oxidation states. Metals in the lower right quadrant stabilize the M−O bond; thus negative potentials are required for the M−O reduction. Reaction 2 is thermodynamically unfavorable on metals in the upper left quadrant. These metals form less stable M−O bonds that are comparatively easier to reduce as shown by the positive reduction potentials for reaction 3.

The information in Figure 2 can provide a starting point for understanding which metals will thermodynamically provide a good surface for oxygen reduction. Based on the data shown in Figure 2, we propose to couple a good oxygen bond cleaving

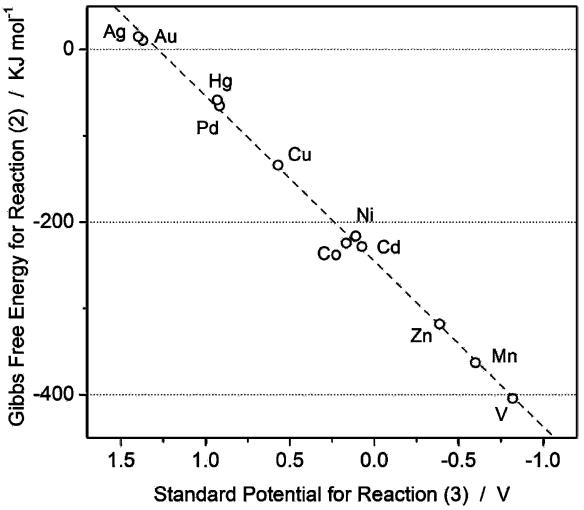

Figure 2. Graph of the Gibbs free energy for reaction 2 versus the standard potential for reaction 3. See text for details.

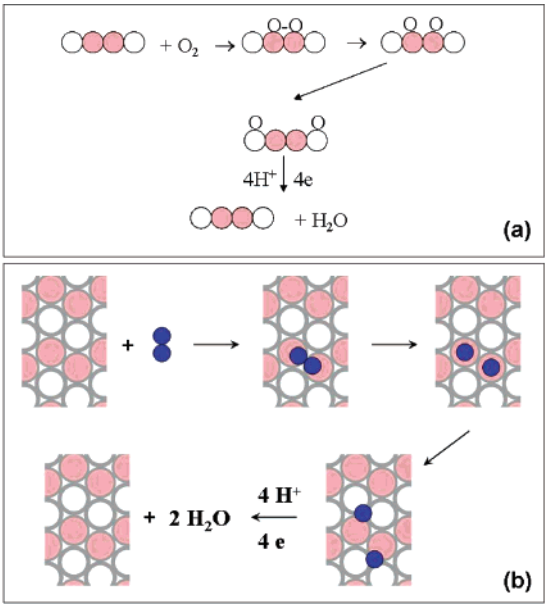

Figure 3. (a) Proposed synergetic mechanism for enhanced electrocatalysis using bimetallic surfaces. (b) Top view schematic of the proposed mechanism. Large pink circles represent good oxygen bond cleaving metal atoms (M). Grey circles represent metal atoms that reduce adsorbed oxygen efficiently (M′). Small blue circles represent oxygen atoms.

metal (M) with a second metal (M′) that is more efficient (i.e., occurs at a more positive potential) for adsorbed oxygen atom (M′O) reduction. A bimetallic alloy system is required where O can migrate from M to M′ where reduction will occur. A schematic of the process is illustrated in Figure 3a. One might question why the O would migrate from the more stable oxide to the less stable one. However, in the proper nanoscale system, migration from the A-top site of M to a 3-fold site involving M′ would be possible (Figure 3b), since oxygen could be more stable in such a 3-fold site.[12]

Note that this model is by its nature a very approximate one, especially since it relies solely on the thermodynamics of a bulk oxide. Clearly, the thermodynamics are different on the surface of a metallic phase and are certainly different in alloys. In addition, the assumption of perfect, intimate contact between different metal atoms within the surface is central in this model

(22) Zurilla, R. W.; Sen, R. K.; Yeager, E. B. *J. Electrochem. Soc.* **1978**, *125*, 1103.
(23) Bard, A. J.; Faulkner, L. R. *Electrochemical Methods*; Wiley: New York, 2001; p 499.
(24) Taylor, R. J.; Humffray, A. A. *J. Electroanal. Chem.* **1975**, *64*, 85.
(25) Clouser, S. J.; Huang, J. C.; Yeager, E. *J. Appl. Electrochem.* **1993**, *23*, 597.
(26) *Standard Potentials in Aqueous Solutions*; Bard, A. J., Parsons, R., Jordan, J., Eds.; Marcel Dekker: New York, 1985.
(27) *Encyclopedia of Electrochemistry of the Elements*; Bard, A. J., Ed.; Marcel Dekker: New York, 1973.

of oxygen electrocatalysis by bimetallic surfaces and implies excellent mixing or alloy formation. Nevertheless, we feel it provides a useful guide to selection of metals to test as electrocatalysts for the ORR.

Results and Discussion

Catalyst Preparation and Morphology. Based on the data illustrated in Figure 2, we have selected a series of metals that ought to provide good surfaces for the reduction of adsorbed atomic oxygen (Ag, Pd, and Au). These pure metals are individually poorly active for electroreduction of oxygen (Ag < Au < Pd) and yield a significant amount of hydrogen peroxide as subproduct.[28−30] This is expected from our hypothesis, since the first step in the direct route, the surface adsorption-splitting of oxygen, is thermodynamically unfavorable on these metals. To ensure intimate contact of metals, it is important to choose metallic combinations that are completely miscible. For example, the model predicts that a combination of Ag and Cu may provide a good surface thermodynamically for oxygen electroreduction. However, Ag and Cu are completely immiscible at room temperature[31] suggesting that no enhancement would be observed, and this has been confirmed by SECM (described in a later section). On the other hand, since most of the metal oxides in the lower right quadrant dissolve rapidly in acidic solutions, especially in the presence of O_2, alloying them into a stable phase is important to avoid dissolution under these conditions. The metal we have selected to provide a good surface for the initial molecular oxygen bond breaking is Co. We have chosen to combine Pd and Co as this combination has recently been shown to exhibit high activity for O_2 electroreduction,[32] approaching that of platinum. In these experiments, each of the alloys studied exhibited excellent stability over the experimental time scale and no significant corrosion of Co was visually observed, although pure Co corroded rapidly. Although Ag and Au are both poor oxygen reduction electrocatalysts, combinations of these two metals with Co were also employed in this study as systems to demonstrate the applicability of our approach. It is known that these metals form stable solid solutions with Co.[31,33] Using our dispenser device, we prepared arrays that contain Pd, Ag, or Au admixed with Co of different compositions. In each spot of the array, the total number of moles of the metal salts used was maintained constant. Scanning electron micrographs of typical arrays of catalyst spots consisting of various amounts of Pd and Co are shown in Figure 4. Figure 4a shows a binary mixture of Pd and Co. The rows consist of pure Pd spots (left) and increasing quantities of Co (10%, 20%, 30%...) (all percentages given are atomic percent) to pure Co spots on the right. Each row was replicated 3 times forming a rectangular array. By repeating the deposition of each column, it was possible to examine the intra-array reproducibility of each catalyst spot preparation. The versatility of our modified plotter-picodispenser technique is illustrated in Figure 4b. It is possible to construct ternary arrays of metallic catalysts over a wide range of compositions. This array consists of pure Au (top), pure Pd (bottom right), and pure Co (top) with a wide range of mixtures of each metal in the intervening areas. Using the picodispenser technique, good reproducibility between spots was observed and little variation was observed between spots of the same composition when using the same preparation procedure. However, the addition of 20% glycerol to each dispensing solution was necessary to ensure a suitable solution viscosity for reproducible spot deposition. The addition of glycerol also prevented the spots from drying before addition of the second (Co) solution. Each spot within an array was typically of the order of 200 μm in diameter. Spots of each of the three metals examined (Pd, Co, Au) exhibited considerably rough morphologies, consisting of dispersed particles with particle sizes in the range 100−200 nm, as determined by SEM. Energy-dispersive X-ray mapping of each metallic combination showed a relatively uniform distribution of the metals across each spot. In this analysis there is a concern about the effect of certain physical parameters affecting the measurements. In particular, the real surface area and the particle size are known to significantly affect the apparent electrocatalytic activity of materials.[34] From the measurements described here, it is impossible to separate

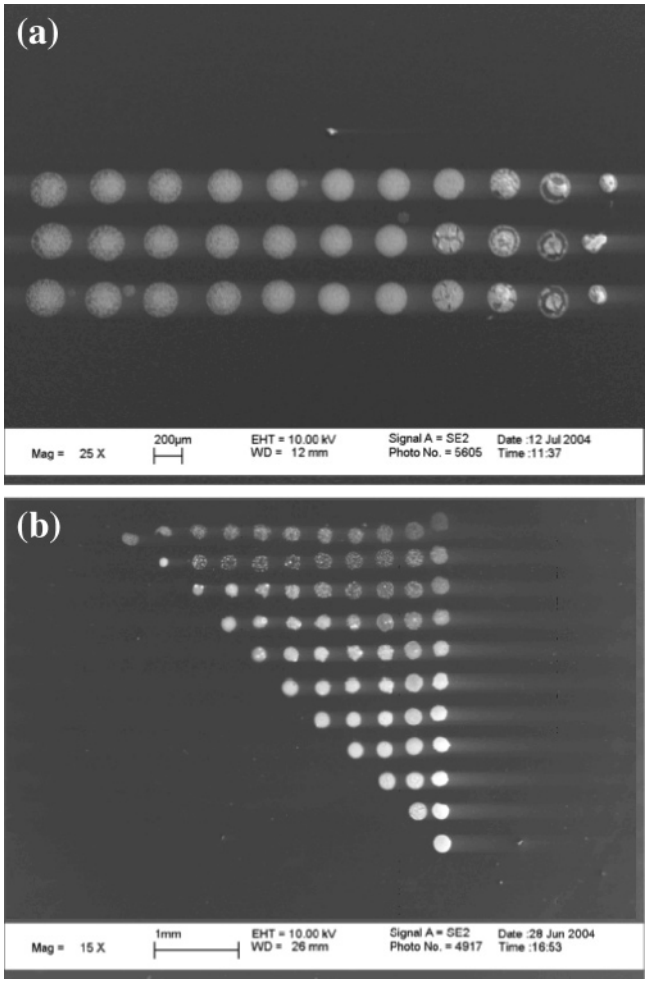

Figure 4. SEM images of typical binary (a) and ternary (b) catalyst arrays. (a) Pd−Co; (b) Pd−Au−Co.

(28) Appleby, A. J. *J. Electroanal. Chem.* **1970**, *27*, 325.
(29) Sepa, D. B.; Vojnovic, M. V.; Vracar, L. M.; Damjanovic, A. *Electrochim. Acta* **1987**, *32*, 129.
(30) Sawyer, D. T.; Day, R. J. *Electrochim. Acta* **1963**, *8*, 589.
(31) *Binary Alloy Phase Diagrams*; Massalski, T., Okamoto, H., Subramanian, P. R., Kacprzak, L., Eds.; ASM International: Ohio, 1990.
(32) Savadogo, O.; Lee, K.; Oishi, K.; Mitsushima, S.; Kamiya, N.; Ota, K.-I. *Electrochem. Commun.* **2004**, *6*, 105.
(33) (a) Noronha, F. B.; Schmal, M.; Fréty, R.; Bergeret, G.; Moraweck, B. *J. Catal.* **1999**, *186*, 20. (b) Mallát, T.; Szabó, S.; Petró, J.; Mendioroz, S.; Folgado, M. A. *Appl. Catal.* **1989**, *53*, 29. (c) Shan, Z. S.; He, P.; Moore, C.; Woollam, J.; Sellmyer, D. J. *J. Appl. Phys.* **1993**, *73*, 6057. (d) Hubin, M.; Garrault, C.; Gouault, J.; Monnaye, B. *Thin Solid Films* **1979**, *58*, 353.
(34) Antoine, O.; Bultel, Y.; Durand, R. *J. Electroanal. Chem.* **2001**, *499*, 85.

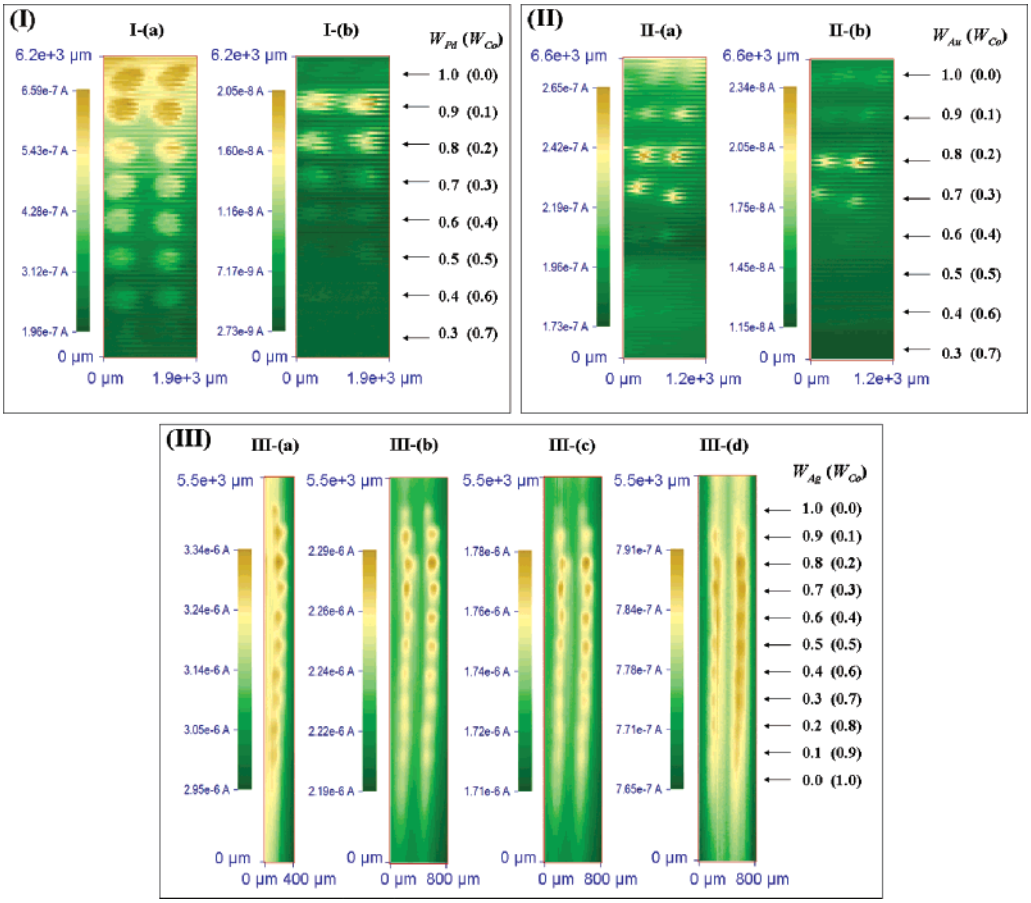

Figure 5. SECM TG-SC images of oxygen reduction activity measured on binary arrays in 0.5 M H_2SO_4. Tip−substrate distance = 30 μm, tip current = −160 nA. (I) Pd−Co, scan rate = 50 μm each 0.2 s, E_S = 0.4 (I-a), 0.7 (I-b) V vs HRE; (II) Au−Co, scan rate = 50 μm each 0.2 s, E_S = 0.2 (II-a), 0.4 (II-b) V vs HRE; (III) Ag−Co, scan rate = 20 μm each 0.017 s, E_S = −0.05 (III-a), 0.05 (III-b), 0.15 (III-c), 0.2 (III-d) V vs HRE. W_M is the atomic ratio of metal M in the spot.

the contribution of each of these parameters from that of the intrinsic activity. However, particle size effects are commonly present only in particles smaller than 10 nm.[35] Thus, it is unlikely that this particle size effect would be observed in materials obtained by reduction of precursors with hydrogen at high temperature, since this method leads to large particle sizes.[36] In addition, the material porosity can affect these measurements, as occurs in RDE and ultramicroelectrode-based experiments. A porous electrode will have an apparent activity much higher than the same smooth material, as evidenced by a decrease in the overpotential for a given apparent current density.[37] We minimized this effect by preparing and testing all of the materials under identical conditions, ensuring minimal variations in the roughness factors between spots. This approach is supported by SEM measurements, in which little variation in the morphology of spots at different compositions was observed.

SECM Activity Imaging and Characterization. The constant tip current TG-SC SECM mode was used to image the electrocatalytic activity of the arrays. Unlike the feedback mode, the TG-SC approach is more appropriate for imaging the activity of rough surfaces, since it is less sensitive to changes in the tip−substrate distance.[38] SECM images of a Pd−Co array recorded at substrate potentials of 0.4 and 0.7 V vs HRE are shown in Figure 5I-a and 5I-b, respectively. At a substrate potential of 0.4 V, each Pd−Co combination exhibits activity for the ORR (up to 70% Co). When the substrate potential is increased to more positive potentials to 0.7 V, the 90:10 Pd/Co composition clearly showed the highest oxygen reduction activity. At this substrate potential, pure Pd exhibited no activity, while catalyst compositions containing more than 20% Co exhibited oxygen reduction activity that decreased with increasing concentrations of Co.

Improvement of the electrocatalytic activity of Au upon addition of Co is also illustrated in Figure 5II-a and 5II-b. At substrate potentials of 0.2 and 0.4 V, 70:30 Au−Co exhibited enhanced electrocatalytic activity for oxygen reduction when compared to each of the other Au−Co combinations. Figure 5III shows the SECM images recorded for Ag−Co catalysts over a range of substrate potentials. At the most negative potential studied (E = −0.05 V vs HRE), Ag and all Ag−Co combinations are clearly equally as active as catalysts for the ORR. However, as the substrate potential was systematically adjusted toward more positive potentials (0 V < E vs HRE < 0.2 V), the Ag activity decreased to zero while a range of the Ag−Co mixtures still retained their activity. The highest activity was observed at a Ag:Co ratio of 80:20. Nonetheless, Au−Co and Ag−Co provide poorer electrocatalytic surfaces than Pd−

(35) Santra, A. K.; Goodman, D. W. In *Catalysis and Electrocatalysis at Nanoparticle Surfaces*; Wieckowski, A., Savinova, E. R., Vayenas, C. G., Eds.; Marcel Dekker: New York, 2003; pp 281−309.
(36) Stonehart, P.; Zucks, P. A. *Electrochim. Acta* **1972**, *17*, 2333.
(37) Paulus, U. A.; Wokaun, A.; Scherer, G. G.; Schmidt, T. J.; Stamenkovic, V.; Markovic, N. M.; Ross, P. N. *Electrochim. Acta* **2002**, *47*, 3787.
(38) Fernández, J. L.; Bard, A. J. *Anal. Chem.* **2004**, *76*, 2281.

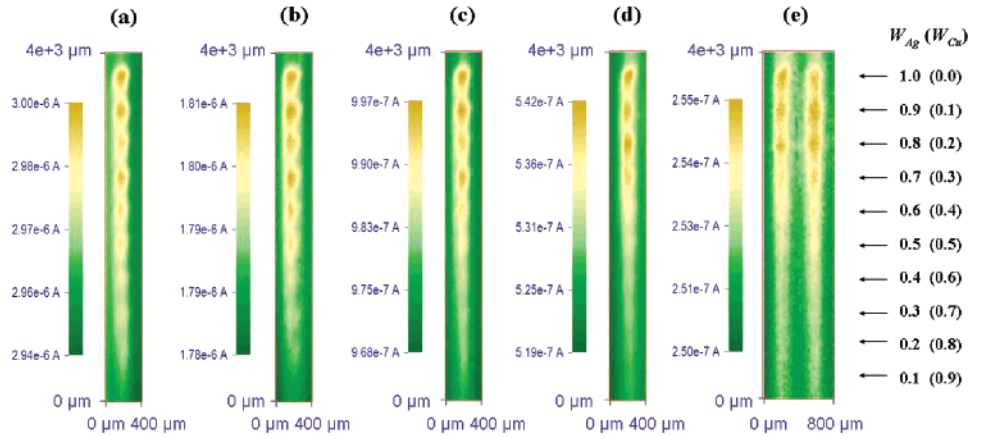

Figure 6. SECM TG-SC images of oxygen reduction activity measured on binary arrays of Ag−Cu in 0.5 M H_2SO_4. Tip−substrate distance = 30 μm, tip current = −160 nA, scan rate = 20 μm each 0.017 s, E_S = 0.0 (a), 0.05 (b), 0.1 (c), 0.15 (d), 0.2 (e) V vs HRE. W_M is the atomic ratio of metal M in the spot.

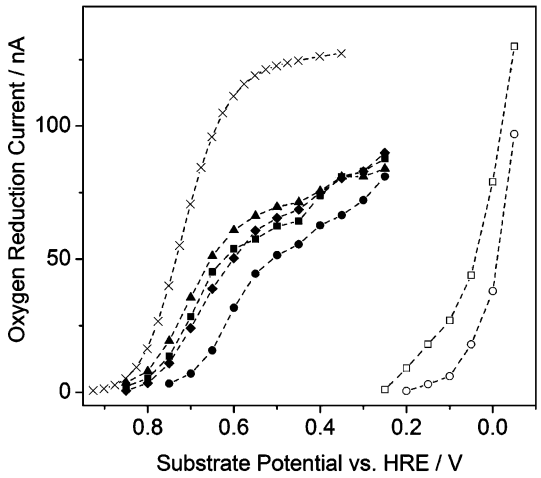

Figure 7. SECM TG-SC polarization curves obtained on individual spots of Pd−Co (solid symbols) and Ag−Co (open symbols) catalysts in 0.5 M H_2SO_4. Tip current = −160 nA. Pd−Co combinations: at. % Pd = 100 (●), 90 (■), 80 (▲), 70 (◆); tip−substrate distance = 50 μm. Ag−Co combinations: at. % Ag = 100 (○), 80 (□); tip−substrate distance = 30 μm. Smooth Pt 100-μm disk (×); tip−substrate distance = 50 μm.

Co, or even pure Pd. However, the observed enhancement of the electrocatalytic activity of Au and Ag upon alloying with Co is significant and tends to support the proposed model.

As mentioned previously, the miscibility of the chosen metals is crucial in the application of this model to choosing electrocatalytic surfaces. Ag and Cu are completely immiscible at room temperature, and therefore, we would expect to see no enhancement of the electrocatalytic activity of silver or copper upon mixing. This was confirmed in an SECM screening of a Ag−Cu array, as shown in Figure 6. Unlike that observed for the Ag−Co combinations, it is not possible to detect any improvement of the activity of Ag−Cu spots with respect to pure Ag. At 0.2 V, samples with less than 30% Cu exhibited a very slight current response during SECM screening.

A more quantitative approach toward monitoring the improved electrocatalytic activity is through current−potential ($i-E$) curves measured on each individual spot using the SECM technique.[20,38] We have constructed $i-E$ curves for a range of Pd−Co and Ag−Co catalysts (Figure 7). Addition of Co to pure Pd catalysts causes a shift in the entire Pd curve toward more positive potentials, indicating more efficient electrocatalysis. The highest activity is observed of all the catalyst mixtures studied at a Pd−Co ratio of 80:20, with an observed shift of the $i-E$ curve of approximately 150 mV. Similarly, an improvement of the catalytic performance of Ag is shown in this diagram. Addition of 20% Co to Ag results in a shift of the $i-E$ curve in an positive direction by approximately 100 mV. As a reference point, included in this diagram is the curve obtained for a smooth Pt electrode under identical conditions. Clearly, the electrocatalytic behavior observed for these catalytic systems does not compete with that of Pt.

In addition to bimetallic mixtures, we probed the effect of trimetallic combinations as catalysts for O_2 reduction to see if the activity and stability was changed by addition of a third metal. Figure 8 shows SECM images of an array containing combinations of Pd, Co, and Au recorded at four different substrate potentials. At the least positive potentials a range of catalyst compositions containing large amounts of Pd showed good activity for oxygen reduction, while catalysts that have high Co contents did not exhibit any electrocatalytic activity. As the substrate potential is shifted to more positive potentials ($\sim$ 0.7 V), a smaller number of catalyst compositions retained electrocatalytic activity (typically Pd mixtures containing 10% Co). At 0.75 V the highest activity was observed for catalyst compositions containing 70% Pd, 10% Co, and 20% Au.

RDE Characterization. Using the SECM screening technique, we have identified a range of catalyst compositions that exhibit enhanced electrocatalytic activity when compared with the pure metals, even at relatively positive potentials. However, the appropriateness of rapid screening techniques to identify novel electrocatalytic materials has been questioned, since such screening techniques employing deposited arrays of metallic catalyst spots do not necessarily provide an accurate insight into the electrocatalytic performance of materials when they are immobilized on electrodes that approach true fuel cell configurations.[39] To test this with the materials studied here, we have used classical RDE experiments to compare the electrocatalytic activities obtained with those observed using the SECM technique. Figure 9 shows $i-E$ curves obtained for a series of Pd−Co catalysts supported on carbon black. The onset potential for oxygen reduction at Pd clearly shifted in the positive

(39) Chan, B. C.; Liu, R.; Jambunathan, K.; Zhang, H.; Chen, G.; Mallouk, T. E.; Smotkin, E. S. *J. Electrochem. Soc.*, in press.

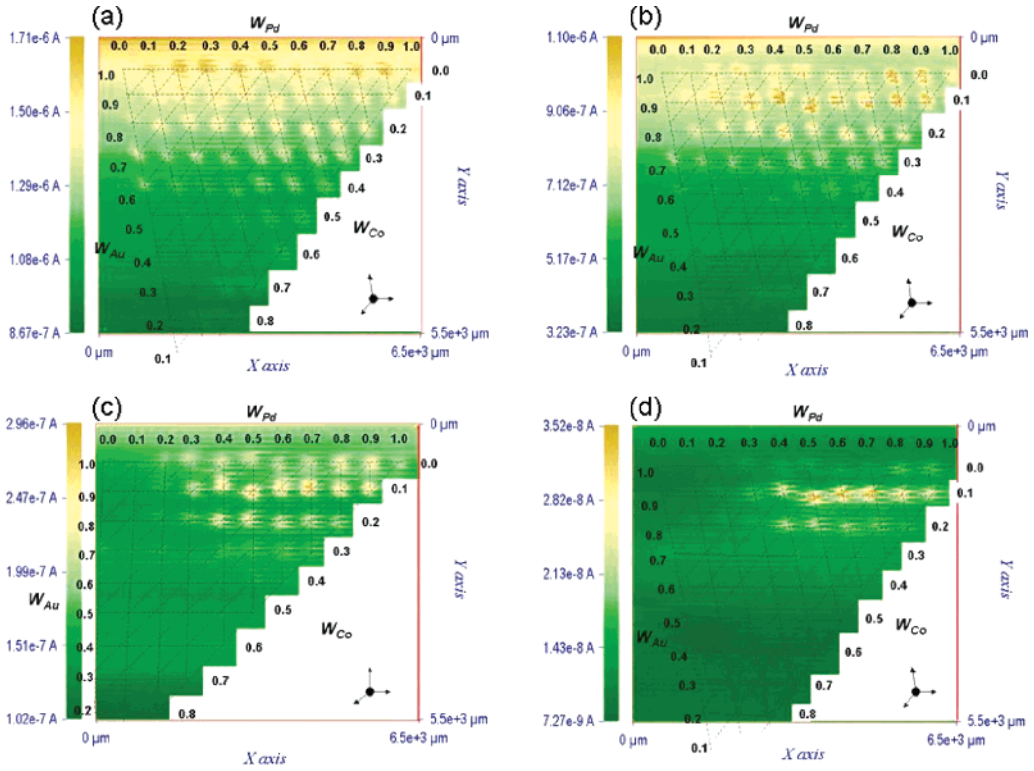

Figure 8. SECM TG-SC images of oxygen reduction activity measured on Pd−Au−Co arrays in 0.5 M H_2SO_4. Tip−substrate distance: 30 μm, tip current = −160 nA, scan rate = 50 μm each 0.2 s, E_S = 0.2 (a), 0.4 (b), 0.6 (c), 0.75 (d) V vs HRE. W_M is the atomic ratio of metal M in the spot.

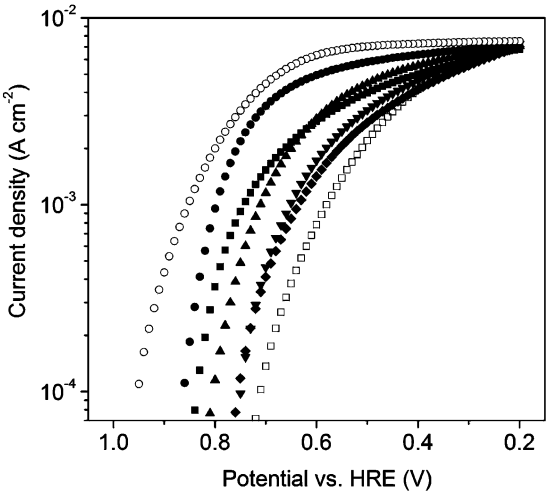

Figure 9. Polarization curves measured by slow potentiodynamic scans (10 mV s^{-1}) of carbon black-supported Pd−Co (20 wt. %) rotating disk electrodes in O_2-saturated (1 atm) 0.5 M H_2SO_4. Rotation rate: 2000 rpm. at. % Pd = 100 (□), 90 (■), 80 (●), 70 (▲), 60 (▼), 50 (◆). Carbon black-supported Pt (20 wt. %) (○).

direction upon addition of Co by about 0.2 V. A mixture of 80:20 Pd−Co clearly exhibited the highest activity, very close to the activity exhibited by Pt, as shown in the screening studies. However, the good performance of Pd−Co was lost after approximately 3 h of continuous operation, as evidenced by a noticeable increase of the ORR overpotential (not shown). Upon addition of 10% Au to the Pd−Co mixture, the stability was greatly improved and the electrode retained its high electrocatalytic activity. Significantly, the agreement between RDE and SECM results is excellent. By comparing the activities determined by both techniques, we have attributed the apparent high electrocatalytic activity of Pd−Co−Au observed in the SECM imaging to a stabilizing effect of Au.

The agreement between the observed enhancement of Pd−Co (by SECM and RDE) with that previously observed using a voltammetric method[32] is remarkable, especially since, in the latter case, the catalysts were prepared by sputtering of the pure metals. In each of the three experiments, the electrocatalytic material was prepared using a different approach, yet the synergetic effect of Co on Pd is apparent in each experiment.

An important issue to address in future studies of these systems is the detection of reaction products, particularly of hydrogen peroxide. This is particularly important if these catalysts are to be considered efficient, alternative electrode materials in polymer electrolyte fuel cells. Furthermore, the absence of hydrogen peroxide as a product would constitute evidence supporting our proposed synergetic scheme, since it will show the "activation" of the direct pathway. We plan to explore the ability of SECM, widely used for detection of reaction products, for hydrogen peroxide analysis from the individual spots. One must also test these catalysts in an actual PEMFC configuration. Such studies are under way.

Conclusion

We have described a simplified scheme for oxygen reduction based on simple thermodynamic principles that can provide guidelines to the design of binary (and multicomponent) electrocatalytic materials. This model involves combining one metal that will easily break the O−O bond of O_2 (forming adsorbed atomic oxygen) with another metal that will easily reduce the adsorbed atomic oxygen. We applied this selection guide to choose and rapidly test by SECM bi- and trimetallic electrode materials. We have prepared arrays of catalysts on carbon substrates and examined the electrocatalytic activity of

each catalyst for the ORR. The SECM technique allows us to rapidly screen the activity of a wide range of catalyst compositions. For each of the metals examined (Ag, Au and Pd), addition of 10 to 20% Co resulted in enhanced electrocatalytic activity. In the case of Pd−Co catalysts, addition of Au appears to increase the stability of the catalyst mixture. As a parallel measurement, we have used classical RDE experiments to examine the electrocatalytic activity of the most promising binary systems, Pd−Co. Significantly, the results obtained using the RDE are in agreement with those obtained using the rapid screening SECM technique. While the electrocatalysts described here do not surpass, or even equal, the activity of platinum surfaces, this approach of combining various metals may allow the development of new and improved electrocatalysts for the ORR in acidic media.

Acknowledgment. This work has been supported by grants from the National Science Foundation (CHE 0109587) and the Robert A. Welch Foundation. J.L.F. thanks the Fundación Antorchas (Argentina) for a postdoctoral fellowship.

JA0449729